Vacuum 84 (2010) 315–320

Contents lists available at ScienceDirect

Vacuum

journal homepage: www.elsevier.com/locate/vacuum

Influence of contact geometry on hardness behavior in nano-indentation

Min Li [a], Weimin Chen [b,*], Yang-Tse Cheng [c], Che-Min Cheng [d]

[a] School of Aeronautic Sciences and Technology, Beijing University of Aeronautics and Astronautics, Beijing 100191, China
[b] Division of Engineering Science, Institute of Mechanics, CAS, Beijing 100190, China
[c] Materials and Processes Laboratory, General Motors Research and Development Center, Warren, MI 48090, USA
[d] State Key Laboratory of Nonlinear Mechanics (LNM), Institute of Mechanics, CAS, Beijing 100190, China

ARTICLE INFO

Article history:
Received 23 February 2009
Received in revised form
29 June 2009
Accepted 3 July 2009

Keywords:
Indenter tip roundness
Surface roughness
Hardness
Nano-indentation

ABSTRACT

In this paper the influence of contact geometry, including the round tip of the indenter and the roughness of the specimen, on hardness behavior for elastic-plastic materials is studied by means of finite element simulation. We idealize the actual indenter by an equivalent rigid conic indenter fitted smoothly with a spherical tip and examine the interaction of this indenter with both a flat surface and a rough surface. In the latter case the rough surface is represented by either a single spherical asperity or a dent (cavity). Indented solids include elastic perfectly plastic materials and strain hardening elastic–plastic materials, and the effects of the yield stress and strain hardening index are explored. Our results show that due to the finite curvature of the indenter tip the hardness versus indentation depth curve rises or drops (depending on the material properties of the indented solids) as the indentation depth decreases, in qualitative agreement with experimental results. Surface asperities and dents of curvature comparable to that of the indenter tip can appreciably modify the hardness value at small indentation depth. Their effects would appear as random variation in hardness.

1. Introduction

Instrumented nano-indentation has provided valuable information on the mechanical property of materials in very small size in bulk or as thin films and coatings. This modeling of indentation was originally based on continuum mechanics regarding materials as homogeneous and without internal structure. Commercial nano-indentation systems usually employ pyramidal indenters such as the Berkovich and Vickers indenters. Ideally each of these indenters yields hardness values independent of the indentation depth in indenting homogeneous elastic–plastic materials. In practice it is commonly found that at small indentation depth of the order of several tens of nanometers or more the nano-indentation measurement system yields hardness value which tends to rise and deviate more and more from being constant as the indentation depth decreases. This phenomenon known as size effect [1–4] in indentation has been the subject of a large number of studies. On one hand, the variation in hardness at small indentation depth is explained by internal material structures such as strain gradient plasticity theories and dislocation density model [5–8] at very small size. On the other hand some authors attributed the variation of hardness to the surface chemical effects such as an oxidation [9], material property variation with depth such as surface work-hardened layer [10] and the error of area function [11]. This paper examines how contact geometric factors, i.e. tip roundness and specimen surface roughness may influence hardness behavior at small indentation depth.

Real indenters are never ideally pyramidal since the tips are always blunt. This by itself introduces at least one linear scale in the mechanics of indentation [12–15]. Surface roughness has also been looked at as another geometric factor [16–20]. Hardness behavior by an indenter with round tip against typical flat elastic perfectly plastic solids has been studied in authors' previous work [15]. In this paper the materials of indented solids are extended to being elastic-plastic, and the influences of material properties including yield stress and strain hardening index are explored. We idealize the actual indenter by an equivalent rigid conic indenter fitted smoothly with a spherical tip and examine the interaction of this indenter with both a flat surface and a rough surface. In the latter case the rough surface is represented by either a single spherical asperity or a dent (cavity). Surface adhesion will be neglected.

Finite element simulation is carried out for elastic-plastic materials with a range of yield stress and hardening index. Hardness as a function of indentation depth is computed. Our results show that at small indentation depth hardness value is no longer constant because of tip roundness and surface roughness. And hardness behavior depends on material parameter, i.e. non-dimensional yield stress σ_Y/E (σ_Y is the yield stress and E is the Young's modulus) and strain hardening index n. For example, for

* Corresponding author. Tel.: +86 010 82543891; fax: +86 010 82338527.
E-mail address: wmchen@imech.ac.cn (W. Chen).

0042-207X/$ – see front matter © 2009 Elsevier Ltd. All rights reserved.
doi:10.1016/j.vacuum.2009.07.001

solid with low value of yield stress σ_Y/E and strain hardening index n hardness rises to a maximum value and then decreases to a constant value corresponding to the value by an ideally self-similar sharp indenter as indentation depth increases, whereas for solid with high value of yield stress σ_Y/E and strain hardening index n hardness rises monotonously and then approaches the constant value due to an ideally self-similar sharp indenter as indentation depth increases. Our results also show that surface asperities and dents of curvature comparable to that of the indenter tip can appreciably modify the hardness value at small indentation depth. Their effects would appear as random variation in hardness.

The plan of this paper is as follows: in Section 2 results of finite element simulation of the indentation of an idealized indenter into a half space are presented to show the effect of the tip radius on hardness. Section 3 shows the finite element simulation results of the indentation of a rigid spherical indenter tip indenting an asperity and a cavity to show to what extent their relative curvature may affect hardness values. Section 4 contains our principal conclusions.

2. Indentation by an idealized conical indenter with a spherical cap

In this section we first examine the problem of an idealized indenter composed of a cone of semi apex angle 70.3° fitted smoothly to a spherical cap of radius R indenting homogeneous elastic–plastic materials. It is known that such an indenter can simulate the Berkovich indenter at large indentation depth. The specimen is assumed to have an ideally flat surface. This idealized indenter is shown schematically in Fig. 1. We note that for contact depth $h_c \le R(1-\sin\vartheta) = 0.059R$, the indentation problem is identical to that of a rigid sphere indenting a flat specimen [21,22].

For such indenters acting on a general elastic–plastic material characterized by the Young's modulus E, yield stress σ_Y, Poisson ratio ν and hardening index n, dimensional analysis [23,24] requires that the hardness H can be expressed as

$$H = Ef\left(\frac{h}{R}, \frac{\sigma_Y}{E}, \nu, n, \vartheta\right), \vartheta = 70.3^\circ \tag{1}$$

The indentation depth corresponding to $h_c/R = 0.059$ (h_c is contact depth) will be denoted by h_s.

From Eq. (1) we know that in addition to the indentation depth h/R and semi apex angle ϑ, material parameters, i.e. σ_Y/E, ν, n affect hardness behavior. In this paper Poisson ratio ν and semi apex angle ϑ are taken to be 0.3 and 70.3° respectively. And the influence of material parameters, non-dimensional yield stress σ_Y/E and strain hardening index n, on the behavior of indentation hardness will be explored.

2.1. Effect of yield stress σ_Y/E on hardness

The finite element calculations are performed using the commercial finite element code ABAQUS. Details of the formulation can be found in the ABAQUS theory manual [25]. The typical mesh for finite element models are shown in Fig. 2. Four-node rectangular elements and three-node triangular elements are used. Finer meshes are employed near the region of contact in order to achieve satisfactory accuracy. A refined mesh is used to obtain better resolution in the elastic regime, for example the mesh spacing is one-third of that of the of the standard mesh.

Finite element simulations are carried out on four elastic perfectly plastic materials that are assumed to be isotropic and homogeneous, where the real contact area is taken, by identifying the surface node coming into contact and then obtaining the contact radius, to calculate the hardness. The yield stress over Young's modulus ratios, σ_Y/E, of two materials is equal to 0.003 and 0.0001 respectively. These two materials exhibit pile-up behavior. The other two materials have values of σ_Y/E ratios equal to 0.1 and 0.01 respectively and exhibit sink-in behavior. For each material, numerical computation is carried out for two rigid indenters of the ideal shape shown in Fig. 1, one has a tip radius of 50 nm and another one has a tip radius of 400 nm. Observing Eq. (1) we note that the hardness H depends on the non-dimension indentation depth h/R, when the material parameters σ_Y/E, ν, n and indenter apex angle ϑ have been taken to be known values. So the finite element predictions of hardness H are plotted against indentation depth h/R in Fig. 3a–d respectively for a range of σ_Y/E (0.0001, 0.003, 0.01, 0.1).

The hardness behavior of the four materials has a common feature. As the indentation depth increases from zero hardness increases and reaches a maximum value. It then decreases and approaches asymptotically a limiting value equal to the hardness due to an ideally sharp conical indenter as indentation depth becomes sufficiently large. This behavior of hardness deviating from constant values is due to the effect of tip roundness of indenter and it was studied in the previous work [15].

In order to explore the influence of relative yield stress σ_Y/E on the hardness behavior, we examine the plot of relative hardness H/H_0 versus indentation depth h/R and the curves (only the results for tip radius of indenter $R = 400$ nm are displayed) are shown in Fig. 4. H_0 is the hardness of ideally sharp conical indenter, or the limiting value of hardness when round tip radius R of indenter approaches zero. As required by Eq. (1) H_0 remains constant for given values of semi apex angle and material parameters. It is seen that for material with low value of σ_Y/E hardness reaches a higher

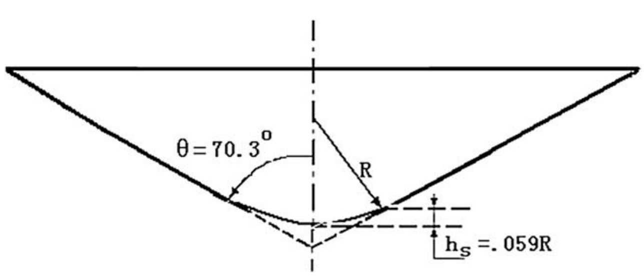

Fig. 1. The ideal indenter – conic indenter with a spherical cap.

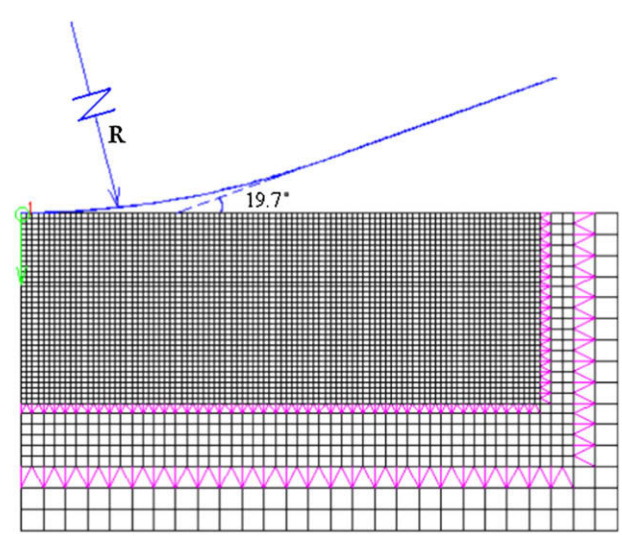

Fig. 2. Typical finite element mesh, composed of four-node rectangular elements and three-node triangular elements.

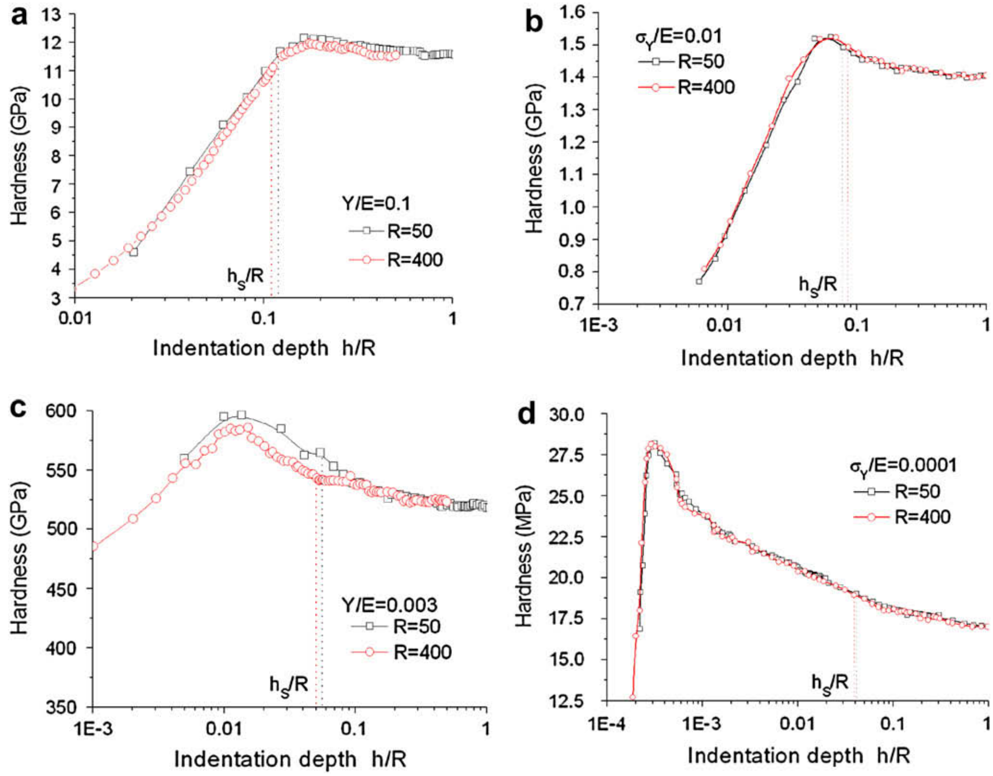

Fig. 3. Computed hardness versus indentation depth h/R using the ideal indenter indenting materials with divergent value of yield stress σ_Y/E (here $n = 0$). a. $\sigma_Y/E = 0.1$; b. $\sigma_Y/E = 0.01$; c. $\sigma_Y/E = 0.003$; d. $\sigma_Y/E = 0.000$.

peak value at a smaller indentation depth. For example, the relative hardness H/H_0 for a material with $\sigma_Y/E = 0.0001$ reaches the peak value, 1.72, at indentation depth $h/R = 3.5 \times 10^{-4}$. And when $\sigma_Y/E = 0.1$ the relative hardness H/H_0 reaches the peak value, 1.06, at indentation depth $h/R = 2.0 \times 10^{-1}$. That is to say, the peak value of H/H_0 increases as the yield stress decreases. The initial increase of hardness with indentation depth was observed by experimental studies [26]. Since for materials with low values of σ_Y/E the maximum hardness is reached at an indentation depth smaller than $h_s = 0.059R \approx 10$ nm, hardness measurements should be done at very small indentation depth so as to observe this part of the

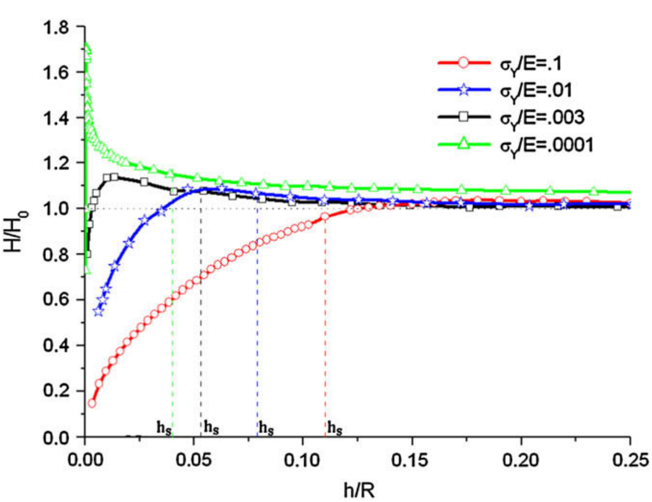

Fig. 4. Effect of σ_Y/E on hardness at small indentation depth.

hardness versus indentation depth curve. So we may say that scale effect of indentation hardness is more pronounced for materials with low values of relative yield stress.

2.2. *Effect of strain hardening index* n *on hardness*

Practical engineering materials strain harden in the plastic range, in this section we will explore the effect of strain hardening index on the indentation response. Here it is assumed that beyond the elastic limit the deformable material satisfies J_2 flow theory with isotropic hardening, and with the total strain obeying a piecewise linear/power law. In uniaxial tension, the stress σ is related to the strain ε by following formulas

$$\sigma = \begin{cases} \varepsilon E & \text{for} \quad \varepsilon \le \sigma_Y/E \\ \varepsilon^n \overline{\sigma} & \text{for} \quad \varepsilon \ge \sigma_Y/E \end{cases} \tag{2}$$

where n is strain harden index, $\overline{\sigma}$ is the strength coefficient, and to ensure continuity the equation $\overline{\sigma} = \sigma_Y (E/\sigma_Y)^n$ should be satisfied.

In finite element simulations the hardening index n of the deformable materials is taken to be 0.0, 0.01, 0.1, 0.2, 0.3, 0.4 and 0.5, and yield stress σ_Y/E is taken to be 0.01, 0.003 and 0.0001 respectively. The indenter tip radii are 50 nm and 400 nm. The influence of hardening index n on the hardness is explored, and selected results of finite element prediction are shown in Fig. 5a–c (tip radius of indenter is $R = 400$ nm) by plotting relative hardness H/H_0 against non-dimension indentation depth h/R. We can see that at large indentation depth the hardness value approaches a constant value, i.e. $H/H_0 \to 1$, but at small indentation depth hardness behaves very differently.

Generally speaking, the value of the hardening index n influences the behavior of the relative hardness H/H_0 versus the non-dimensional indentation depth h/R curve in a significant way.

Taking hardness behaviors for material with $\sigma_Y/E = 0.003$ (shown in Fig. 5b) as an example, we can see that for the material with a high value of n, e.g. $n = 0.5$ and 0.2, at small indentation depth values of relative hardness are always smaller than 1.0, or the hardness H at smaller depth is always smaller than the hardness at larger indentation depth. That is to say, the curves of hardness versus depth are monotonic and do not have peaks. However, for the material with a low value of n, e.g. $n = 0.0$ and 0.01, at small indentation depth the relative hardness increases and reaches a peak value exceeding the value of 1.0. For elastic perfectly plastic material ($n = 0.0$ and $\sigma_Y/E = 0.003$) the maximum value, $H/H_0 = 1.15$ is reached at depth $h/R = 9.8 \times 10^{-3}$.

It is also seen that higher peaks of hardness occur at smaller indentation depth. And the highest peak corresponds to $n = 0$, namely when the material is elastic perfectly elastic. This behavior of hardness at small indentation depth can be observed in experimental results [2,17,26]. Considering the initial increase of hardness at indentation depth much smaller than h_s may easily be missed in hardness measurements, we may say that the size effect for material with low value of hardening index is more pronounced.

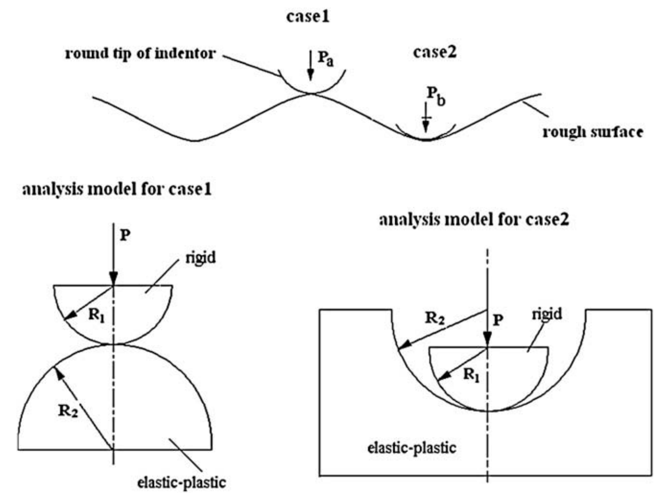

Fig. 6. Schematics of the contact geometry of a rigid sphere with: 1) another sphere, 2) a spherical cavity.

3. Indenting a sphere and cavity by a rigid sphere of radius R_1

Real surfaces are never flat so that the initial contact of the indenter with the specimen surface will be either with an asperity of positive curvature $1/R_2$ or, if the tip of the indenter is sharp enough, with a cavity of negative curvature $-1/R_2$. In this section we model this situation by the contact between a rigid sphere of radius R_1 with a deformable sphere of radius R_2 and with a deformable spherical cavity of radius R_2 (shown in Fig. 6). Again, the material being indented is taken to be elastic perfectly plastic with yield stress $\sigma_Y/E = 0.003$.

The contact problem between elastic spheres was first solved by Hertz. A similarity solution for elastic–plastic contact has been given by Storaker et al. [27]. But its range of application is too restricted for the present purpose. Numerical simulation to deal with larger plastic deformation was done by Mesarovic and Fleck [21,22] in their study of compaction of spherical pellets. The present paper extends their results to contact between two spheres and between a sphere and a cavity. For more information readers may refer to Refs. [28–30].

Similar to Eq. (1) hardness in this case can be expressed functionally as

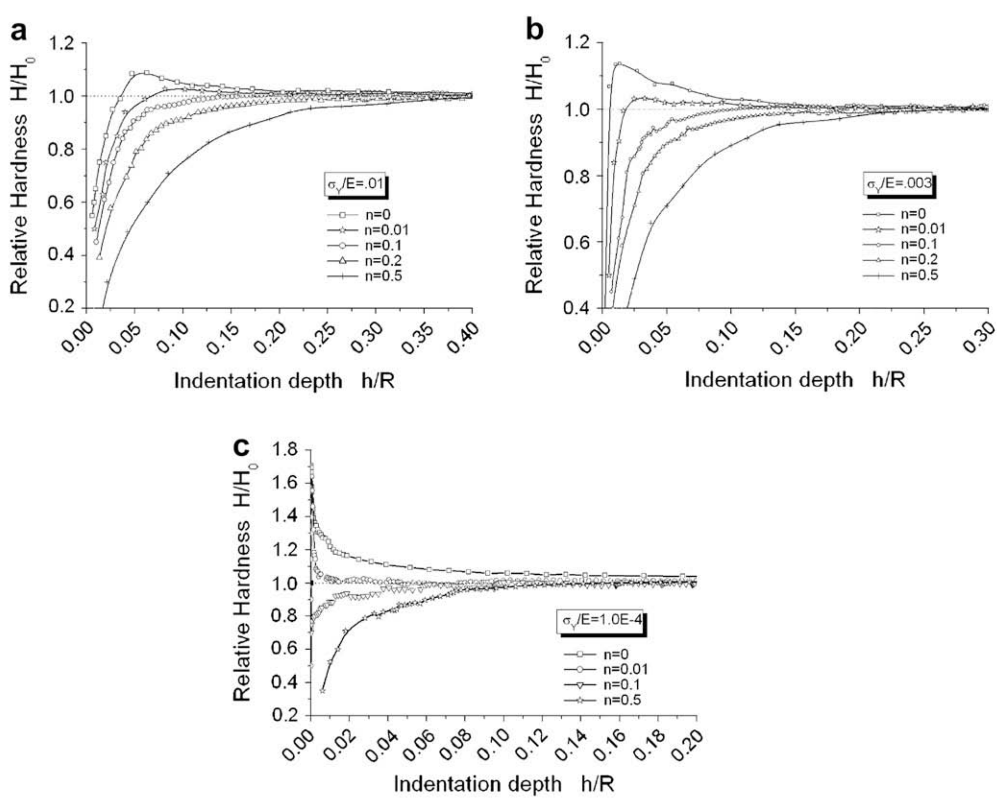

Fig. 5. Computed hardness versus indentation depth h/R using the ideal indenter indenting strain hardening materials. a. $\sigma_Y/E = 0.01$; b. $\sigma_Y/E = 0.003$; c. $\sigma_Y/E = 0.0001$.

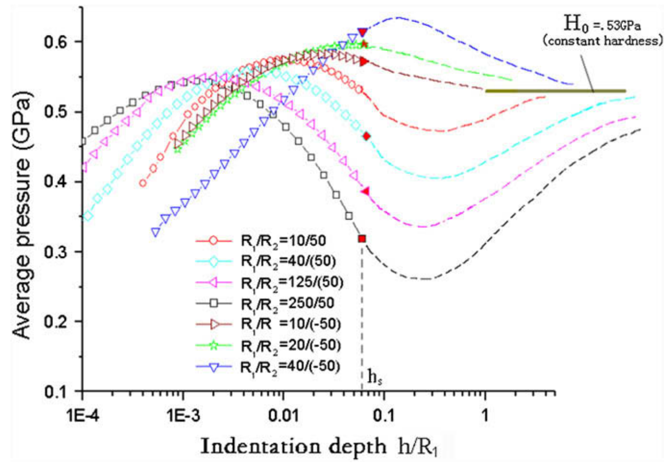

Fig. 7. Computed hardness versus indentation depth between a rigid sphere (R_1) and either a spherical (R_2) asperity or a spherical cavity ($-R_2$).

$$H = Ef\left(\frac{h}{R_1}, \frac{\pm R_2}{R_1}, \frac{\sigma_Y}{E}, \nu, n, \vartheta\right) \quad (3)$$

where the plus sign applies to contact between spheres and the negative sign applies to the contact between sphere and cavity.

In Fig. 7 hardness is plotted against the indentation depth for a range of the parameter $\pm R_1/R_2$. The indentation depth h_s below which the sphere/sphere and sphere/cavity models simulate the contact of the ideal sphere capped indenter discussed in the last section is marked in the figure by fully filled symbols. In the case of the ideal indenter discussed in the last section, hardness must approach a limiting value for indentation depth much larger than h_s. This limiting value H_0 is also shown in Fig. 7.

An interesting feature of the curves in Fig. 7 is that the hardness values for indentation depth below h_s can either be significantly lower or higher than H_0 depending on the algebraic value of the ratio $\pm R_1/R_2$. This means that surface roughness can appreciably alter the hardness readings of instrumented indentation measurement in a random manner. Another interesting observation is that the value of H relative to H_0 and the sign of the slope of the hardness/indentation depth curve at h_s in Fig. 7 may introduce additional new features such as peaks and dips in the hardness versus indentation depth curves at depth beyond h_s. It is also of interest to note that at the indentation depth $h/R \approx 0.06$, the concept of reduced radius R^* lumping the two parameters h/R_1 and R_2/R_1 into a single h/R^* no longer applies. At small indentation depth or for problem of small deformation, based on Hertz contact theory, the radii of two contacting spheres appear only in the combination $(1/R_1)+(1/R_2)$ in the formulation of the contact problem, it can be replaced by a single parameter $(1/R^*)=(1/R_1)+(1/R_2)$, R^* is known as the effective radius. But at large indentation depth ($h/R \approx 0.06$), the concept of reduced radius R^* no longer applies because of large deformation. Based on dimension analysis (Eq. (3)) two non-dimensionless parameters h/R_1 and R_2/R_1 are needed.

4. Conclusions

In this paper the influence of contact geometry, including the round tip of the indenter and the roughness of the specimen, on hardness behavior for elastic-plastic materials is studied by means of finite element simulation. Our results show the following:

1. Due to the finite curvature of the indenter tip the curves of hardness versus indentation depth rise or drop as the indentation depth decreases. Scale effect is more pronounced for materials with low values of yield stress and hardening index. Indentation measurement at small depth is influenced by many factors, therefore hardness value at very small indentation depth should be used carefully.
2. Asperities and dents on the surface of the test specimen can cause further changes in hardness values at small indentation depth. This can be a cause of random scatter in experimental measurements at small indentation depth.
3. In order to extract material property from indentation tests at small indentation depth, it is necessary to first remove the effects of geometric factors such as those studied in this work from the indentation data.

Acknowledgement

The authors would like to acknowledge support from the National Science Foundation of China, project nos. 10772183 and 10532070.

References

[1] de Guzman MS, Neubauer G, Flinn PA, Nix WD. The role of indentation depth on the measured hardness of materials. Mater Res Symp Proc 1993; 308:613–8.
[2] Ma Q, Clarke DR. Size dependent hardness of silver single crystal. J Mater Res 1995;10:853–63.
[3] Poole WJ, Ashby MF, Fleck NA. Micro-hardness of annealed and work-hardened copper polycrystals. Scripta Mater 1996;34:559–64.
[4] Feng G, Nix WD. Indentation size effect in MgO. Scripta Mater 2004;51: 599–603.
[5] Saha R, Xue Z, Huang Y, Nix WD. Indentation of a soft metal film on a hard substrate: strain gradient hardening effects. J Mech Phys Solids 2001; 49:1997–2014.
[6] Begley MR, Hutchinson JW. The mechanics of size dependent indentation. J Mech Phys Solids 1998;46:2049–68.
[7] Nix WD, Gao H. Indentation size effects in crystalline materials: a law for strain gradient plasticity. J Mech Phys Solids 1998;46:411–25.
[8] Huang Y, Xue Z, Gao H, Nix WD, Xia ZC. A study of micro-indentation hardness tests by mechanism-based strain gradient plasticity. J Mater Res 2000;15:1786–96.
[9] Gerberich WW, Venkataramanan SK, Huang H. The injection of plasticity by millinewton contacts. Acta Metall Mater 1995;43(4):1569–76.
[10] Liu Y, Ngan AHW. Depth dependence of hardness in copper single crystals measured by nanoindentation. Scripta Mater 2001;44:237–41.
[11] Chen W, Li M, Xu X. Comments on the calibration technique of the projected contact area of nano-indentation tester. Chin J Theor Appl Mech 2005;37(5):645–52 [in Chinese].
[12] McElhaney KW, Vlassak JJ, Nix WD. Determination of indenter tip geometry and indentation contact area for depth-sensing indentation experiments. J Mater Res 1998;13:1300–6.
[13] Swadener JG, George EP, Pharr GM. The correlation of the indentation size effect measured with indenters of various shapes. J Mech Phys Solids 2002;50:681–94.
[14] Iwashita N, Swain MV. Elastic-plastic deformation of silica glass and glassy carbons with different indenters. Philos Mag A 2002;82:2899–906.
[15] Chen WM, Li M, Zhang TH, Cheng YT, Cheng CM. Influence of indenter tip roundness on hardness behavior in nanoindentation. Mater Sci Eng A 2007;445–446:323–7.
[16] Bhushan B. Contact mechanics of rough surfaces in tribology: single asperity contact. Appl Mech Rev 1996;49:275–98.
[17] Bobji MS, Biswas SK. Deconvolution of hardness from data obtained from nanoindentation of rough surfaces. J Mater Res 1999;14(6):2259–68.
[18] Bobji MS, Biswas SK. Effect of roughness on the measurement of nanohardness – a computer simulation study. Appl Phys Lett 1997;71(8):1059–61.
[19] Zhang TY, Xu WH. Surface effect on nanoindentation. J Mater Res 2002;17:1715–20.
[20] Zhang TY, Xu WH, Zhao MH. The role of plastic deformation of rough surfaces in the size-dependent hardness. Acta Mater 2004;52:57–68.
[21] Mesarovic SD, Fleck NA. Spherical indentation of elastic–plastic solids. Proc R Soc London A 1999;455:2707–28.
[22] Mesarovic SD, Fleck NA. Frictionless indentation of dissimilar elastic–plastic spheres. Int J Solid Struct 2000;37:7071–91.
[23] Cheng YT, Cheng CM. Scaling, dimensional analysis, and indentation measurements. Mater Sci Eng R 2004;44:91–149.
[24] Cheng YT, Cheng CM. Scaling relationships in conical indentation of elastic–perfectly plastic solids. Int J Solid Struct 1999;36:1231–43.

[25] HKS, Inc. ABAQUS manual. Pawtucket, RI, USA, 2005.
[26] Lee KW, Chung YW, Chan CY. An international round-robin experiment to evaluate the consistency of nanoindentation hardness measurement of thin film. Surface Coat Technol 2003;168:57–61.
[27] Storaker B, Biwa S, Larsson PL. Similarity analysis of inelastic contact. Int J Solid Struct 1997;34:3061–83.
[28] Zhao Y, Maietta DM, Chang L. An asperity microcontact model incorporating the transition from elastic deformation to fully plastic flow. Trans ASME 2000;122:86–93.
[29] Kogut L, Etsion I. Elastic–plastic contact analysis of a sphere and a rigid flat. J Appl Mech 2002;69:363–71.
[30] Jackson RL, Green I. A finite element study of elastic–plastic hemispherical contact against a rigid flat. J Tribol 2005;127:343–54.